Video Article

Designing Silk-silk Protein Alloy Materials for Biomedical Applications

Xiao Hu[1,2,3], Solomon Duki[1], Joseph Forys[1], Jeffrey Hettinger[1,2], Justin Buchicchio[1], Tabbetha Dobbins[1,2], Catherine Yang[2,4]

[1]Department of Physics and Astronomy, Rowan University

[2]Department of Biomedical and Translational Sciences, Rowan University

[3]Department of Biomedical Sciences, Cooper Medical School of Rowan University

[4]Department of Chemistry and Biochemistry, Rowan University

Correspondence to: Xiao Hu at hu@rowan.edu

URL: http://www.jove.com/video/50891
DOI: doi:10.3791/50891

Keywords: Bioengineering, Issue 90, protein alloys, biomaterials, biomedical, silk blends, computational simulation, implantable electronic devices

Date Published: 8/13/2014

Citation: Hu, X., Duki, S., Forys, J., Hettinger, J., Buchicchio, J., Dobbins, T., Yang, C. Designing Silk-silk Protein Alloy Materials for Biomedical Applications. *J. Vis. Exp.* (90), e50891, doi:10.3791/50891 (2014).

Abstract

Fibrous proteins display different sequences and structures that have been used for various applications in biomedical fields such as biosensors, nanomedicine, tissue regeneration, and drug delivery. Designing materials based on the molecular-scale interactions between these proteins will help generate new multifunctional protein alloy biomaterials with tunable properties. Such alloy material systems also provide advantages in comparison to traditional synthetic polymers due to the materials biodegradability, biocompatibility, and tenability in the body. This article used the protein blends of wild tussah silk (*Antheraea pernyi*) and domestic mulberry silk (*Bombyx mori*) as an example to provide useful protocols regarding these topics, including how to predict protein-protein interactions by computational methods, how to produce protein alloy solutions, how to verify alloy systems by thermal analysis, and how to fabricate variable alloy materials including optical materials with diffraction gratings, electric materials with circuits coatings, and pharmaceutical materials for drug release and delivery. These methods can provide important information for designing the next generation multifunctional biomaterials based on different protein alloys.

Video Link

The video component of this article can be found at http://www.jove.com/video/50891/

Introduction

Nature has created strategies to generate tunable and multifunctional biological matrixes using a limited number of structural proteins. For example, elastins and collagens are always used together *in vivo* to provide the adjustable strengths and functions required for specific tissues[1,2]. The key to this strategy is the blending. Blending involves mixing proteins with specific ratios and is a technological approach to generate simple material systems with tunable and varied properties[3-5]. Compared with synthetic engineering strategies[6,7], blending can also improve material uniformity and the ability to process the material due to the ease of operation[8-16]. Therefore, designing multifunctional, biocompatible protein alloy materials is an emerging area of medical research. This technology will also provide systematic knowledge of the impact of natural protein matrices on cell and tissue functions both *in vitro* and *in vivo*[10,17]. By optimizing molecular interfaces between different proteins, protein-based alloy materials can encompass a range of physical functions, such as thermal stability at different temperatures, elasticity to support diverse tissues, electrical sensitivity in variable organs, and optical properties for corneal tissue regeneration[3,18-27]. The outcome of these studies will provide a new protein-materials platform in the field of biomedical science with direct relevance to tunable tissue repairs and disease treatments and further lead to biodegradable implant devices where their novel therapeutic and diagnostic features can be envisioned[3].

Many natural structural proteins have critical physical and bioactive properties that can be exploited as candidates for the biomaterial matrixes. Silks from different worm species, keratins from hairs and wools, elastins and collagens from different tissues, and various plant proteins are some of the most common structural proteins used for designing variable protein-based materials (**Figure 1**)[18-27]. In general, these proteins can form different molecular secondary structures (*e.g.*, beta sheets for silks, or coiled coils for keratins) due to their unique repetitive primary amino acid sequences[3,28-35]. These features promote the formation of self-assembled macroscopic structures with unique functions at biological interfaces prompting their utility as a treasured resource of biopolymer materials. Here, two types of structural proteins were used (protein A from wild tussah silk and protein B from domesticated mulberry silk as an example) to demonstrate the general protocols of producing various protein alloy biomaterials. The protocols demonstrated include part 1: protein interaction predictions and simulations, part 2: production of protein alloy solutions, and part 3: fabrication of protein alloy systems and for optical, electrical, and pharmaceutical applications.

Figure 1. Raw materials of various structural proteins that are commonly used in our laboratory for designing protein-based materials, including silks from different worm species, keratins from hairs and wools, elastins from different tissues, and various plant proteins.

Protocol

1. Prediction of Protein Interactions

1. Bioinfomatics Analysis of Protein Molecules
    1. Visit the National Center for Biotechnology Information website (www.ncbi.nlm.nih.gov/protein/), and search the protein names that will be used for the alloy study. Note: For this example, two proteins were used: protein A, which is the wild tussah silk fibroin, and protein B, which is the domestic mulberry silk fibroin. For protein A, the amino acid sequences can be found in "fibroin [Antheraea pernyi] GenBank: AAC32606.1" (*Antheraea pernyi* is the Chinese (Oak) Tussah Moth). For protein B, the amino acid sequences can be found in "fibroin heavy chain precursor [Bombyx mori] NCBI Reference Sequence: NP_001106733.1" and "fibroin light chain precursor [Bombyx mori] NCBI Reference Sequence: NP_001037488.1" together (*Bombyx mori* is the domesticated silkworm of the mulberry tree).
    2. Select and save the amino acid sequences of the protein A and protein B from the database.
    3. Visit the ExPASy website (the SIB Bioinformatics Resource Portal) (www.expasy.org) or use other commercial software to calculate the basic bioinfomatics data of proteins based on their sequences including, but not limited to, total charge per molecule, hydrophobicity index of the molecule, titration curve of the molecules at different pH values, etc. This information will be used as basic elements for the computational simulation of protein interactions, and will help to understand whether these two proteins have strong interactions. [Note: This step is not for precisely predicting every detail of the protein interaction like those used in small peptides or functional proteins science. The purpose of this section is only to avoid producing a protein mixture with obvious macrophase separations which cannot be called an "alloy" material. Therefore, the estimate could be approximate but the protein alloy system can be verified by an experimental method described in step 3.1 using precise thermal analysis].

2. Computational Simulation of Protein Alloy system
    Below is described a procedure to simulate the protein alloy system. A simulation program is written in C programming language that can be used on a single or multiprocessor computer system. A lattice-spring-mass (LSM) model was used to simulate the alloy-proteins[36-39]. The LSM model gives a simple description of the net force on a mass when attached to a spring and one can solve the force equation to understand the motion for each mass. A simple program algorithm to model this protein alloy system using the LSM model is given as follows:
    1. Represent a single protein as a coarse-grained particle that has a mass of m.
    2. Use a Hookean or a neo-Hookean spring to represent a bond[38,39]. By interlinking a finite number of particles with springs, one can make a sub-alloy domain that represents a stable building block of the alloy-proteins. To represent different types of bonds in the intra-linkage, use different spring constants/stiffness.
    3. Model the protein alloy system as a material composed of dully-crosslinked sub-alloys. Again here different stiffnesses were used to represent different bonds between inter-linkages of the sub-alloys.
    4. Model the bond breaking and reformation process by a Bell Model[40,41], through which weak bonds are allowed to be reformed but strong bonds cannot reform once they are broken. When the system is sufficiently stressed (both on the intra-suballoy and inter-suballoy bonds), bonds can be broken and reformed.
    5. In order to study deformation effects on the alloy-proteins when they are stressed, apply external forces to the system. Distribute these forces equally to each particle when solving the force equation (The Newton's Laws).

6. To model interactions between the solution (such as water molecules) and the proteins, apply an additional drag force or frictional force to each particle.
7. Solve the force equation for each particle with the actions of each force (the spring force from the bond, the external force, and the frictional force).
8. Calculate and extract the positions of the protein particles as a function of time.
9. Calculate the physical quantities that characterize the alloy-proteins from the positions of the particles.
10. Change the bond stiffness in the program to understand interactions between different proteins. (The average bond stiffness is calculated from the Young's modulus of the protein materials. The Young's modulus of different fibrous protein materials can be obtained either by Universal Tensile Test[18], or directly from previous literatures[2-4,18]).

2. Production of Protein Alloy Solutions

Wild tussah silk (protein A) and domestic mulberry silk (protein B) are selected here as an example of protein alloy system. This protocol first presents how to obtain the wild tussah silk (protein A) solution.

1. Cut raw wild tussah silk cocoons or fibers at a weight of 3 g.
2. Measure 3 g of sodium dicarbonate or sodium carbonate (Note: If using sodium carbonate, the molecular weight of protein chains will reduce during the boiling process[42]).
3. Fill a 2 L glass beaker with distilled water (H_2O). Then, place the glass beaker on a hot stage, cover it with aluminum foil, and heat to boiling.
4. Remove the aluminum foil cover and add the measured sodium dicarbonate slowly into the boiling water, allowing it to completely dissolve. (Note: The role of sodium dicarbonate is the "soap" to clean off soluble sericin proteins and other impurities attached on the surface of wild silk fibers. If using other nature protein fibers, please select corresponding chemical agents according to the literature).
5. Add the raw protein fibers (wild silk fibers) into the boiling water and allow to boil for 2-3 hr (Note: The boiling time has critical impact to the molecular weight of protein chains[26,43]. One should select an appropriate time according to the literature or by performing control experiments[26,43]. The boiling temperature could also be adjusted to impact the molecular weight of the protein chains[26,43,44]).
6. After boiling, carefully remove the protein fibers with a spatula from the solution and squeeze them to remove the excess water. (CAUTION: The fibers are very hot!)
7. Next, immerse the fibers in a 2 L beaker with cold distilled water, and wash the fibers twice for 30 min each to completely remove the impure residues from the fiber surface. Dry the fibers in a fume hood for at least 12 hr.
8. Melt 45.784 g of calcium nitrate ($Ca(NO_3)_2$) in a glass beaker to form a liquid at 65 °C for dissolving the wild silk protein fibers. (Note: If using other natural protein fibers, select a corresponding solvent to dissolve the proteins. Here you can also use 9.3 M LiSCN or LiBr solution, or an 85% phosphate solution for dissolving different silk fibers.)
9. Combine the fibers and the solvent at a ratio of 1 g fiber into 10 ml solvent. Allow the fibers to dissolve at 95 °C for 5 to 12 hr. (Note: The dissolving time depends on the molecular weight of proteins[26,43-45])
10. Using syringes, inject the wild silk solution into 12 ml dialysis cassettes (maximum 1,000 MW as the cutoff size) or sealed dialysis tubings (maximum 1,000 MW as the cutoff size) and dialyze against 2 L of distilled water. (Note: The injection is more efficient if maintaining the solution at 35 °C, otherwise the viscosity of protein solution will dramatically increase at room temperature). Change the distilled water frequently to remove $Ca(NO_3)_2$ solvents in the solution (after 30 min, 2 hr, 6 hr, and then every 12 hr for 3 days. In total, there will be approximately 8 water changes).
11. After 3 days, collect the protein solutions from the dialysis cassettes or tubing and place into 13,000 rpm rated tubes.
12. Centrifuge the solutions for 1 hr at 3,500 rpm at 4 °C 3x to remove deposits. After each centrifuge run, quickly pull the supernatant into new tubes. Store the final solutions in a 4 °C refrigerator.
13. Pour 5 ml of protein solution onto a polydimethylsiloxane (PDMS) substrate or other flat hydrophobic substrate and allow it to dry completely (this usually takes more than 12 hr). Weigh the remaining solid protein film and calculate the final solution concentration by weight percentage (w/v%) = Measured Weight (in mg) ÷ 5 (in ml) ÷ 10.
14. Collect another selected natural protein fiber (in this case, domesticated mulberry silk was used as the protein B), and repeat above process with an appropriate "soap" and dissolving solvent, until the final protein water solution with measured concentration is obtained. [Note: If the protein materials are in the powder form, use appropriate porous tubes or membranes to hold the samples during the "soaping" process. If the protein has already been purified, directly go to step 2.8 to dissolve the powder. If the protein has already been purified and is water soluble, make its aqueous solution with a desired concentration first and then go to step 2.15 below to make blend protein solutions.]
15. Slowly dilute the Protein A solution (here wild silk solution) in distilled water at 4 °C to form a 1.0 wt% Protein A aqueous solution. Do the same process for Protein B (here domesticated silk).
16. Slowly mix the 1 wt% protein A solution with Protein B solution at 4 °C using a pipette to avoid protein aggregation during mixing. (Note 1: Do not use a vortex instrument to mix the proteins since some proteins (*e.g.*, silks) will form hydrogels during the vibration[46,47]. Note 2: If possible, use additional devices to control the mixing rate and mixing size making sure to mix them as slow as possible to avoid aggregation. Do not quickly pipette the solution during mixing).
17. The final blending solutions should have a specified mass ratio or a molar ratio of Protein A:Protein B. Typically, mix them with mass ratio of 90:10, 75:25, 50:50, 25:75, 10:90 to obtain a broad spectrum of alloy solutions. Use pure protein A and protein B solutions as controls. For a blending solution with a molar ratio of Protein A:Protein B = R: (100-R). Calculate the mixing volume ratio (based on a same 1 wt% solution) by: Volume A:Volume B = R·(MW of A): (100-R)·(MW of B).
18. Immediately cast the final solutions on to PDMS substrates to form films or other designed materials. (Note: Do not store high concentration protein alloy solutions for a long time. More aggregates may form later due to the protein-protein interactions in water). If needed, dilute the blend solutions with ion-free distilled water and keep them in a 4 °C refrigerator to avoid additional protein aggregation in solutions.

3. Fabrication of Variable Protein Alloy Materials

1. Confirm Alloy Prediction by Thermal Analysis[3,9,31-35]
    1. Prepare PDMS substrates and clean them by soaking in distilled water.

2. Cast the protein blend solutions with different mixing ratios onto the PDMS substrates.
3. Dry the solutions for at least 12 hr in a chemical hood with air flow until films are formed (Note: Use the same volume for different solutions so that the thickness of films can be fixed).
4. Remove the protein alloy films from the PDMS substrates and place them onto clean dishes.
5. Weigh many Differential Scanning Calorimetry (DSC) aluminum pans and lids for DSC study. Match the pan and lid pairs to have an equal total weight (weight of pan plus weight of lid equals a constant weight). For example, here a total weight of lid and pan 22.50 mg was used, and eight sets of lid and pan combinations with this total weight were prepared.
6. Encapsulate 6 mg each type of dried protein blends into aluminum DSC pans and seal them with their matched lids in process 3.1.5. Seal an empty pan and lid pair to be used with the sample as the reference so that only the heat capacity of samples themselves will be recorded during the thermal analysis (Note: The DSC will compare the heat capacity of reference pan+lid vs. that of sample+pan +lid. Due to the equal weights, the background heat capacity from the pans and lids will be accounted for leaving only the heat capacity of sample in the pan).
7. Put sealed references and sample pans into a DSC instrument, with purged dry nitrogen gas flow of 50 ml/min, and equipped with a refrigerated cooling system. Before the sample measurements, the DSC instrument should first be calibrated with sapphire and indium for heat flow and temperature, respectively.
8. Pre-run the DSC at a heating rate of 2 K/min to 150 °C and then hold at this temperature for 15 min to remove any remaining water molecules in the samples (typically around 3-10% of total weight). Quickly cool down (10 K/min) to 25 °C.
9. Run the DSC again at a heating rate of 2 K/min to 300 °C, or until the degradation peak of protein blends appear[34]. Record the heat capacities of the protein sample at different temperature during this process. Cool down the DSC and change the old sample to a new sample with a different mixing ratio.
10. Calculate and plot the Heat Capacity vs. Temperature curves for each protein blend sample using the DSC software[31-35].
11. Judge the miscibility of protein blends by the following method (See **Figure 4** Thermal and **Figure 5**) and if the two proteins are fully miscible, they may be called “protein alloys”. Otherwise the term “protein composite” would be a suitable name according to polymer descriptive theories[48,49]):
    1. The individual proteins A and B should have individual single glass transitions temperature, T_g(A) and T_g(B) (See the green and blue curves in **Figure 5**)[3,48];
    2. This single glass transition temperature is normally intermediate between those of the two individual protein components, T_g (A) and T_g (B) (See **Figure 5**)[3,48];
    3. Immiscible phase separation blends is obtained if both T_g(A) and T_g(B) appeared at their original positions (**Figure 5**), and with each T_g step height in proportion to the composition, the two proteins are fully immiscible[3,48].
    4. Semi-miscible composite blend type of will have one very broad glass transition, or may still have two glass transitions, but each has migrated closer to each other relative to the pure protein components, T_g(A) and T_g(B) (see **Figure 5**). In this case, there might be micro-heterogeneous phase structures formed between the two protein components, and the composition may vary from location to location.
12. If (3.1.11.1) is the case shown in DSC, and it can be confirmed that the protein A-B is an alloy system, then move on to fabricate protein alloy materials.

2. Fabrication of Optical Materials by Protein Alloys
    1. Produce (in the fabrication lab) or purchase a designed topographic surface for casting. In this specific example, a glass with four diffraction patterns was used (**Figure 4** Optical).
    2. Place the glass with diffraction patterns into a dish, and make sure the patterned surface is faced upward.
    3. Spread PDMS solution evenly on the glass surface, and fully cover the surface patterns (The PDMS solution is made by potting and catalyst solution in a 9:1 mixing ratio according to the user instruction[23,44]).
    4. Place the casting dish into a 65 °C oven for at least 2 hr while on a flat surface. The PDMS solution should dry into a solid substrate during this process.
    5. Remove PDMS substrate from the glass. The diffraction patterns should now be transferred to the PDMS surface.
    6. Punch out the PDMS molds with diffraction patterns using a suitable hole punch.
    7. Drop protein alloy solutions on the PDMS surfaces with diffraction patterns, and dry them for at least 12 hr to obtain films with diffraction patterns.
    8. To obtain insoluble protein alloy materials, place the entire set of dry films, including the PDMS molds into a 60 °C vacuum oven (25 kPa) with a water dish on the bottom of the chamber. Pump out air in the oven, and let the water vapors anneal samples for at least 2 hr. (This process is called temperature-controlled water vapor annealing[45]. Comparing with the widely used methanol method, it can generate similar beta-sheet content in the silk materials[45]). Release the vacuum and peel off the water insoluble film from the PDMS substrate using forceps. For this example, wild silk-domesticated silk alloys are used.
    9. Test the quality of diffraction patterns on films by comparing them with the original patterns on the glass (*e.g.*, collect SEM images for the micro-scale details; collect laser diffraction patterns for the general pattern quality).

3. Fabrication of Electrical Circuits on Protein Alloys Materials
    1. To fabricate an electrical circuit pattern on glass substrate, first clean a glass slide using some degreasing solvent such as Alconox in an ultrasonic cleaner for 5 min, followed by 5 min in acetone, followed by 5 min in methanol. The methanol is used last since it evaporates more slowly than acetone so can be blown off the substrate rather than drying and leaving residues.
    2. Blow the glass slide dry using dry nitrogen gas which is generated by the boil-off from a 180 L liquid nitrogen dewar.
    3. Introduce the substrate materials into the deposition chamber. (These guidelines are for a sputtering system but other deposition techniques could be used.) If the chamber is designed with a loadlock, the vacuum in the deposition chamber is not significantly impacted. Evacuate the loadlock to a pressure of 30 mTorr.
    4. Open the gate valve between the loadlock and the main deposition chamber and introduce the substrate into the chamber.
    5. Turn on the Ar gas and the pressure regulator and control the pressure to the desired deposition pressure. Higher pressures give lower energy sputtered metal atoms and more uniform films while lower pressures yield better adhering faster deposited films. The range of pressures is generally between 3 mTorr and 60 mTorr, with 20 mTorr working well.

6. Metals are then projected onto a shutter that protects the substrate from coating using an RF power of 100 W. A tuning circuit is required to direct the RF power to the metal target. DC power could be used instead of RF for metallic targets. In order to remove oxide layers and contaminants from the target, pre-sputter for several minutes.
7. Open the shutter and sputter the metal onto the substrate. The deposition rate for the configuration described is about 10 nm per min. This rate will depend on working distance, pressure, magnet strength in the magnetron cathode, target thickness and the metal sputtered. Adjust the deposition time to achieve the desired thickness.
8. Remove the coated glass slide from the chamber.
9. Using a spinner, spin a photoresist coating onto the surface of the film. Many resists can be used. For this case, positive photoresist was used.
10. After the resist is spun onto the film, soft bake at 90 °C for 5 min to dry the resist.
11. Place a contact mask with an image of the device firmly against the resist. A UV light source is used to expose the photoresist. The exposure is 10 sec but varies depending on the strength of the light source and the resist used.
12. Place the film in the photoresist developer until the projected image appears. The developer washes away the resist that was exposed to the UV light which cause the breaking of the polymer bonds. Immediately after the image appears, dip the film in DI water to stop the developer from working on the unexposed photoresist.
13. Blow the films dry with dry nitrogen gas.
14. Place the films into an oven at 120 °C for 15 min to “hard bake” the photoresist.
15. After the films cool, place them in an etching solution until the metal not protected by the photoresist lifts off. Dip in water to stop the etching.
16. Rinse with acetone to remove the hardened photoresist.
17. Rinse with methanol and blow dry with dry nitrogen.
18. Once the coated glasses are ready, drop different protein alloy solutions onto the glass surfaces, and dry them for at least 12 hr to obtain protein alloy films on the glasses. (It is suggested to first concentrate the alloy solutions to 5 wt% to obtain thick protein alloy films.)
19. Due to the hydrophobic-hydrophilic interactions, the thin metal films will be transferred from the glass surfaces to the attached protein alloy film surfaces[51]. Peel off the protein alloy films with the thin metal patterns from the glass substrates using forceps.
20. To obtain insoluble protein alloy materials, place the dry films into a 60 °C vacuum oven (25 kPa) with a water dish on the bottom of the chamber. Pump out air in the oven, and let the water vapors anneal samples for at least 2 hr. Release the vacuum and peel off the water insoluble film from the substrate using forceps.
21. Test the electrical qualities of metal patterns on protein alloy films such as electrical resistance and compare them to the original patterns on the glass.

4. Fabrication of Pharmaceutical Materials by Protein Alloys
    1. To fabricate a protein alloy films with pharmaceutical compounds, first prepare a PDMS substrate as described in step 3.2. Clean the formed PDMS substrate by distilled water.
    2. Dissolve or disperse the pharmaceutical compounds into an aqueous solution. Use ultrasound or vortex to homogeneously mix the pharmaceutical compounds with the water. If the compounds are not water soluble, disperse the powders with a homogeneous distribution in the ion-free distilled water.
    3. Calculate the desired mass ratio of compounds to the protein alloys by: volume of compound solution x weight percentage of compound solution : volume of protein alloy solution x weight percentage of compound solution (here 1 wt% alloy solution was used). Select a ratio to obtain a film with desired compound density in the protein alloy film.
    4. Slowly mix the compound solution with the protein alloy solution following the same instructions in section 2 process 2.16. (Note: To avoid gelation, do not ultrasonicate or vortex the solution during the mixing).
    5. Pour a calculated volume of mixture onto the PDMS substrate and dry it at least 12 hr in a chemical hood to a obtain protein alloy film containing a designed ratio of pharmaceutical compounds.
    6. Physically crosslinked the film following the same instruction in Section 3.2 process 3.2.8. An example of alloy films with insoluble model drugs of a low density (LD) or a high (HD) density could be seen in **Figure 4** Chemical.

Representative Results

Typical protein-protein interactions (*e.g.*, between protein A and protein B) could contain charge-charge (electrostatic) attractions, hydrogen bonding formation, hydrophobic-hydrophilic interactions, as well as dipole, solvent, counter ion, and entropic effects between the specific domains of the two proteins (**Figure 2**)[3]. Therefore, fundamentally, we can predict the effects of these interactions by computational simulations.

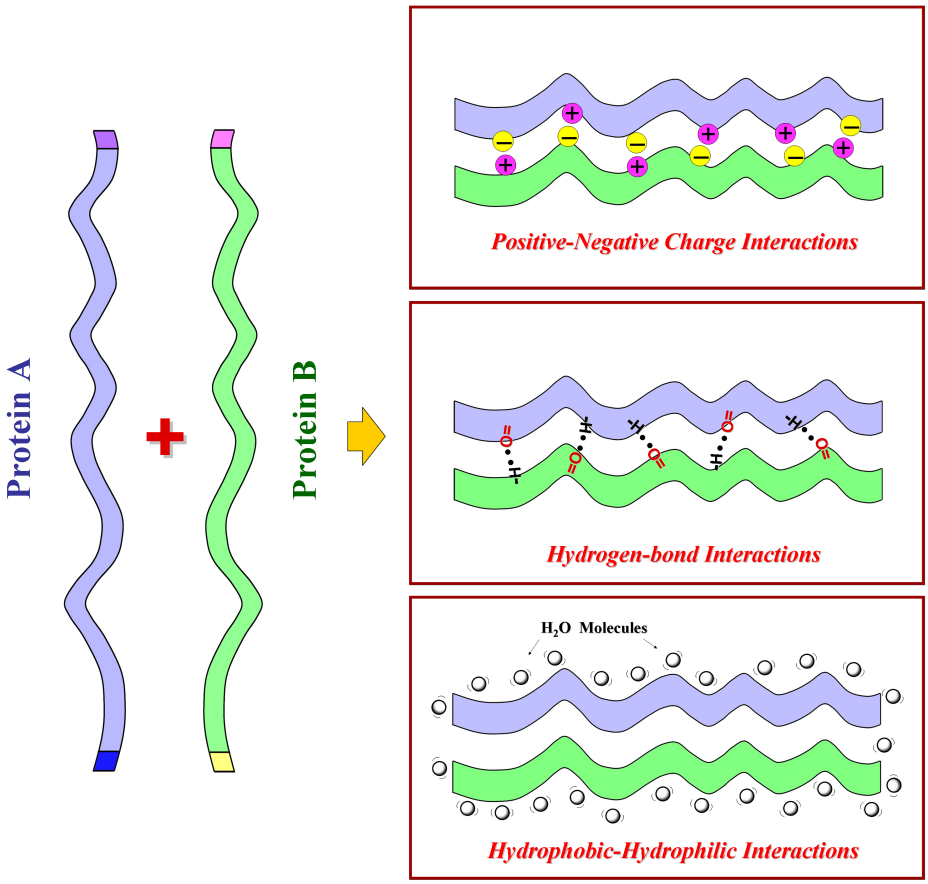

Figure 2. Interactions between protein A and protein B. Typically, these interactions could be based on charge-charge (electrostatic) attractions, hydrogen bonding formation, or hydrophobic-hydrophilic interactions between the specific domains of these two proteins.

The protein-alloy system can be modeled as a material composed of crosslinked protein sub-alloy domains, where each of these sub-alloys is assumed to be stable. The interactions between the proteins (A and B) can be considered as bonds with different stiffnesses (for this study, we consider only two types of weak or strong bonds in **Figure 3**). The weak bonds could represent hydrogen bonds and other bonds described in **Figure 2**. The protein-alloy as a whole is formed through dual cross-linkages between many sub-alloys that bounded together through both strong and weak bonds. The sub-alloys are formed using strong bonds and within the sub-alloys we allow the formation of weaker bonds. The protein-alloy as a whole is formed through dual cross-linkages between many sub-alloys that bound together through various strong and weak bonds. When the system is sufficiently stressed, both the weak and the strong bonds are ruptured. Under right conditions the weak bonds are allowed to reform the linkages again. However, the stronger bonds will be ruptured irreversibly. The existence of the weak bonds allows the alloy-protein to keep its structural integrity under external stress[36-41]. This numerical simulation uses a mathematical model developed through a bottom-up approach that is based on finite element methods through lattice-spring model[36-41].

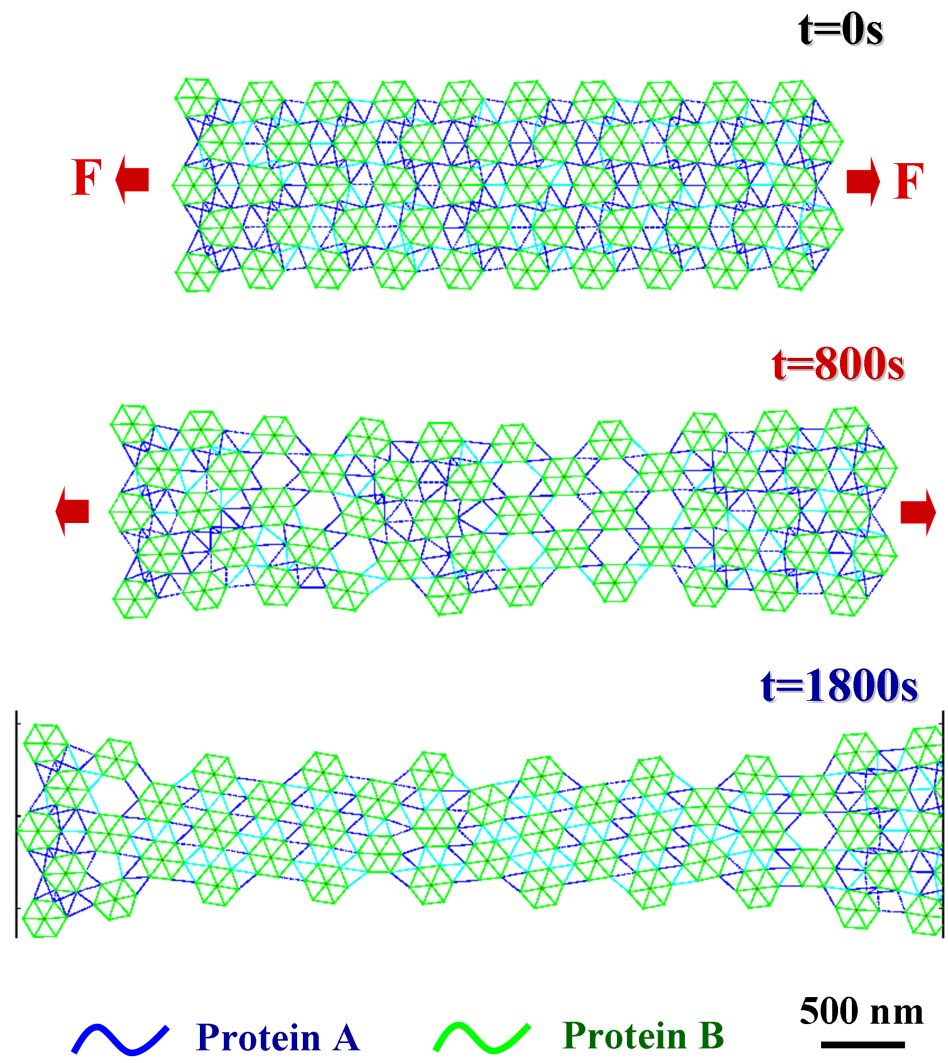

Computational Simulation of Protein Interactions

Figure 3. Computational simulation to demonstrate the mechanical advantage of a protein alloy system during stretching. During the stretching simulation, one type of protein (blue color) can form an elastic network like springs providing super-elasticity for the materials, while another type of protein (green color) can provide strong physical crosslinkers for stabilizing the material network. Dynamic structural transitions (*e.g.*, hydrogen bond formations and deformations) could be induced in different domains for storing and releasing energy or providing additional mechanical support during the stretching.

Figure 3 demonstrates a typical computational simulation of the mechanical properties of a protein alloy system (with wild tussah silk as protein A and domesticated mulberry silk as protein B) during stretching. During the stretching simulation, one type of protein (blue color) can form an elastic network with springs providing super-elasticity for the materials, while another type of protein (green color) can serve as particles with strong physical crosslinkers for the material network. Dynamic structural transitions (*e.g.*, hydrogen bond formation and deformation) can be induced in different domains for storing and releasing energy or providing additional mechanical support during the stretch. The simulation studies gives a general theoretical picture to understand the interactions between different structural protein molecules, such that useful pairs of proteins could be picked to generate protein alloy materials with strong interactions and specific properties, such as extraordinary mechanical elasticity.

Generally, once the protein A and B are selected (here they are wild silk and domesticated silk), a protein alloy solution can be produced in several steps (**Figure 4**). First, the protein sources like natural fibers or powders should be cleaned or purified. For example, a degumming process could be used to remove the soluble silk sericin proteins coated on most silk fibroin fibers[20]. Second, a suitable solvent needs to be found to dissolve the insoluble protein sources into solutions. For instance, high concentration LiBr solution is a good solvent to cut beta-sheet secondary structures in different silks and dissolve the fibers into solutions. Third, a dialysis method can be used to remove the dissolving solvent and recover the protein molecules in an aqueous solution. Additional centrifuging is often necessary to remove the impurities and undissolved aggregates in the solution. Finally, different protein aqueous solutions can be mixed together gently with various ratios. Therefore, if the two protein solutions do not have macrophase separation, they will be blended together with strong interactions and form new protein alloy

system for different biomedical applications. To make the protein alloy materials insoluble in the body, different physical or chemical crosslinking treatments can be adapted. For example, it is found that high-temperature and high-pressure water vapor annealing could incredibly crosslink different silk or elastin materials[6,52]. While different keratin materials can be crosslinked by their natural disulfide bonds in the protein side chains[53].

Once the protein alloy solutions are produced and verified, they can be formed into a wide range of biomaterials with tunable properties, including material matrixes for thermal, mechanical, optical, electrical, chemical, or biomedical applications (**Figure 4**). In this article, three emerging applications for these materials to demonstrate the unique advantage of protein alloy biomaterials have been selected (**Figure 4**). Through modern micro-fabrication techniques, different surface patterns can be generated at micro or nano-scales on protein alloy materials (**Figure 4** optical application). For example, if an optical diffraction pattern is produced on the film surface, this film can used as a media to transfer laser beams into different optical pattern[22,23]. If the protein alloy material was emerged in an enzyme solution, the degradation profile of the films can be understood by comparing the real-time diffraction patterns from the film with the original pattern (instead of back and forth washing and examining the degraded films in the air). Another emerging technique is to coat different micro-scale circuits and wireless resonators on the protein alloy materials (**Figure 4** electrical application). Through this technique, micro-currents of damaged tissues or organs *in vivo* can be monitored, with wireless signals directly transferred to doctors[24,51]. And the material mechanical toughness and biodurability in the body can be easily controlled by blending ratios and specific protein components of the materials. Finally, different soluble or insoluble cancer drugs can be directly incorporated into the protein alloy materials (**Figure 4** chemical application). Cancer drugs are often very toxic, and will damage not only the cancer cells but also the normal human immune system. Therefore, controlling the region and dose of cancer drug delivery per day in the body is one of the most important topics in pharmaceutical science. Through incorporating cancer drugs into protein alloy materials, we can implant the material only into cancer tissues or organs, and control the release rate of the cancer drug per day from protein alloy network by controlling the protein components and mixing ratios. Since the protein matrix is completely biodegradable, the protein alloy materials will be automatically removed by body enzymes after the drug releasing period. The residues of protein alloy materials are purely amino acids, which can be absorbed by the body naturally to further produce other essential proteins *in vivo*. Patients who get cured by controlled release of cancer drugs from implanted protein alloy materials will finally recovered without additives in the body, and both natural protein alloy matrixes and cancer drugs will be efficiently absorbed in the body during this curing process.

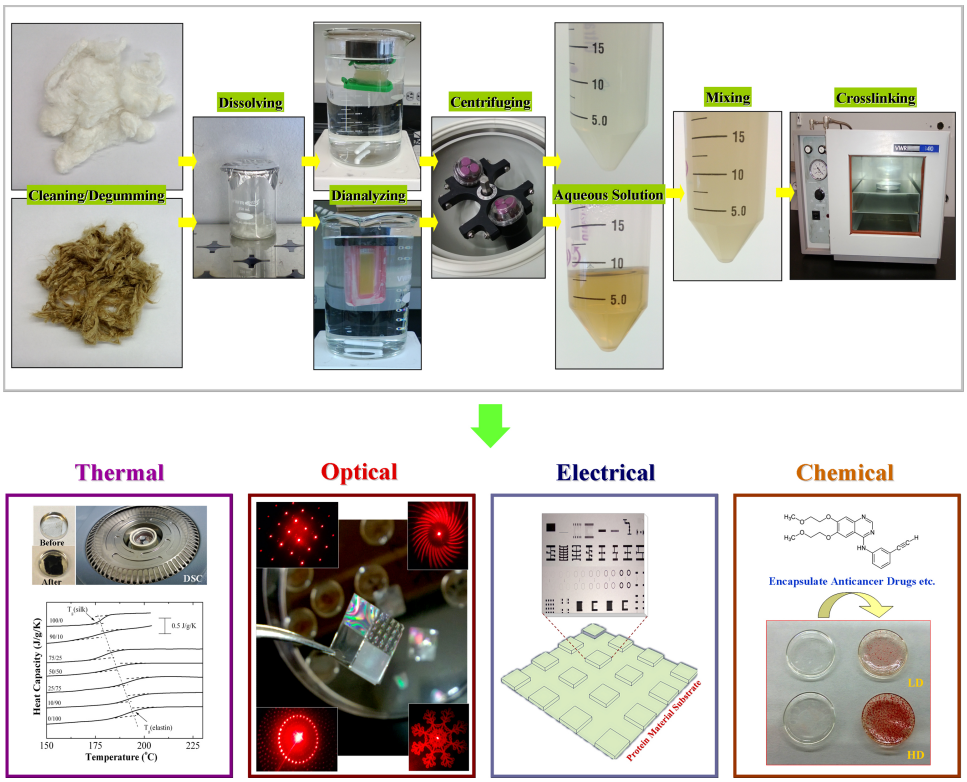

Figure 4. General steps to produce a protein alloy material, including cleaning or purifying the protein material sources, dissolving the insoluble protein materials into solutions, dianalysizing to remove the dissolving solvent from a protein aqueous solution, centrifuging and mixing together with different ratios, and physical or chemical crosslinking treatments. The protein alloy solution can subsequently be formed into a wide range of biomaterials with tunable properties, including material matrixes for thermal, mechanical, optical, electrical, chemical, or biomedical applications. Please click here to view a larger version of this figure.

Here, we demonstrated the critical procedures of how to fabricate electrical materials on protein alloys with details in **Figure 5**. Thin metallic films such as electric circuits can be created using several different deposition techniques including evaporation, pulsed laser deposition, or sputtering. Sputtering was selected for the current study since it offers significant flexibility for the energy of the sputtered species through the adjustment of sputtering gas pressure and power applied to the cathode as well as deposition uniformity through adjustment of the gas pressure and cathode size. Sputter deposition can be used to project a metallic film onto a glass substrate (**Figure 5A**). In this case, Ag circuit films were deposited in a high vacuum chamber with a base pressure of about 1 x 10^{-7} Torr. The Ar sputtering gas was introduced to the chamber at a pressure of 20 mTorr and the Ag was deposited using an RF generator at 100 W for 20 min from a 2-inch planar magnetron cathode that is 8 cm from the

substrate surface. Devices are defined using common photolithographic techniques in the films on glass followed by wet chemical etching (see detailed procedure in **Figure 5A**). Devices can also be defined by deposition through a physical mask directly onto the protein films. The room temperature electrical resistivity of the electric circuits on the protein films was measured using both two-terminal and four-terminal techniques. The advantage of the four-terminal approach is to eliminate contact resistance from the measurement but we find that the contact resistance is not significant so a two-terminal measurement is sufficient. The two terminal measurements uses a good-quality multimeter set on the ohm scale making contact with the film at both ends of the metal wire (schematically shown in **Figure 5B**). In this measurement, the multimeter serves as both a current source and a voltmeter and the measured resistance is the voltage divided by the current. The resistivity is calculated using $\rho = RA/l$, where R is the resistance, A is the cross-sectional area of the wire and l is the distance between probes. For the created here, the R was measured to be 23.5 Ω using the slope of voltage-current curve in **Figure 5B** (R=ΔVoltage/ΔCurrent), l is 4.45 x 10^{-2} m, and A was found to be 6.685 x 10^{-10} m^2. Using these numbers, a resistivity of 3.6 x 10^{-7} Ω·m was found for the films, approximately 20x larger than that for bulk silver metal (1.6 x 10^{-8} Ω·m). A higher resistivity measured in films in comparison to bulk is typical due to the already constrained current path and the inability of charge carriers to avoid defects. Heating the metal with a heat gun increased its resistance indicating an increase in the rate of electron scattering by phonons characteristic of metallic conduction.

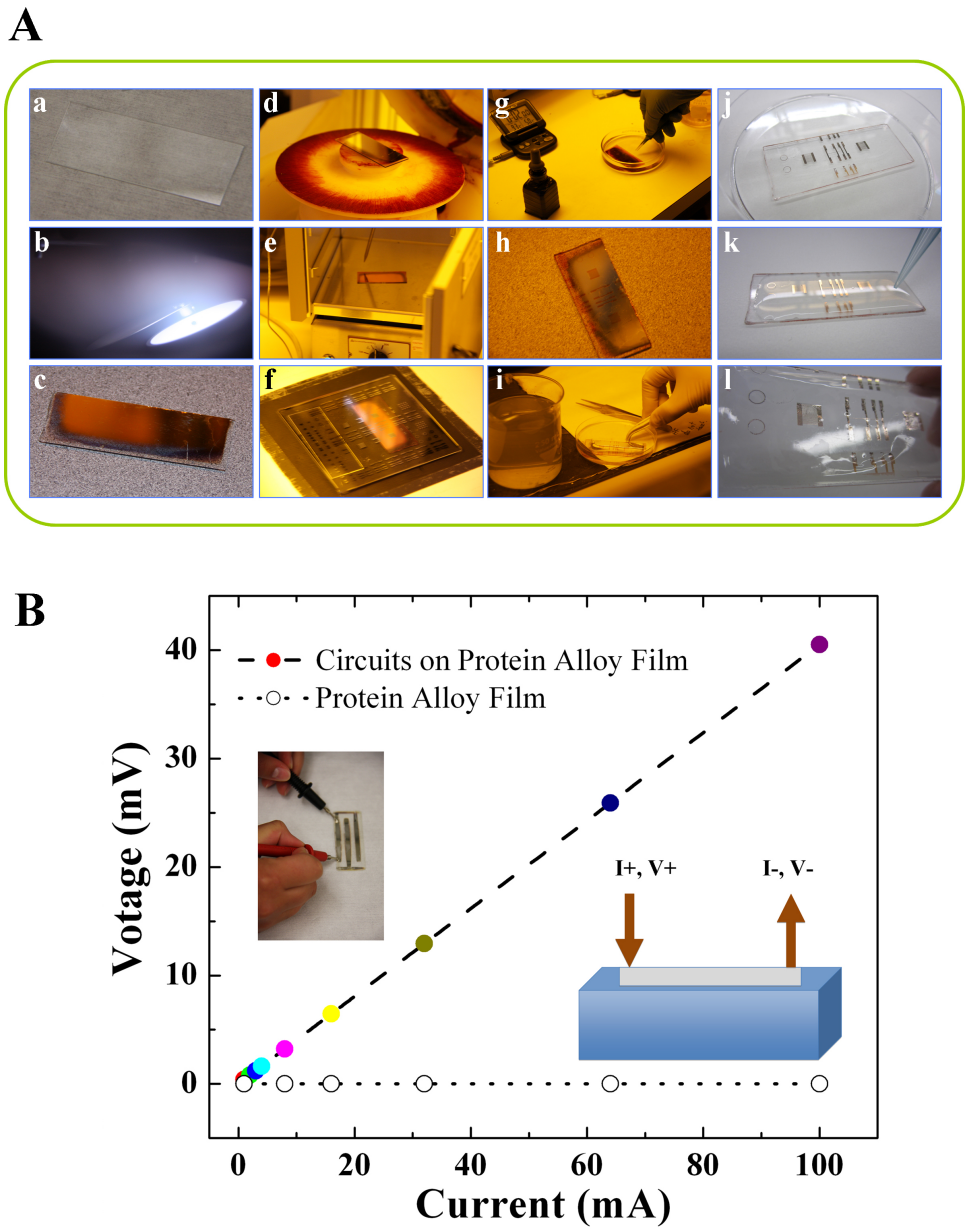

Figure 5. (A) Procedure to make electric circuits on protein alloy films (here silver circuits on wild tussah silk and mulberry silk blend films as an example): (a) Uncoated microscope slide; (b) Silver plasma during sputter deposition from a 2 foot diameter target; (c) Silver coated glass slide; (d) Silver coated sample held to the spinner using the vacuum chuck before adding the photoresist; (e) Silver slide coated with photoresist was put into oven for soft-bake at 120 °C; (f) Expose to UV radiation to break the polymer bonds in the photoresist; (g) Develop the photoresist; (h) Hard-bake the resist to prepare for etching in acid; (i) Etch in the acid, then stop the etch by rinsing in a water bath; (j) Dry the slide; (k) Cast protein alloy solution onto the slide; (l) Transfer silver patterns to the dried protein film. **(B)** A typical voltage-current curve of the produced electric circuits on a protein alloy film. The final electrical resistivity on film is measured around 3.6×10^{-7} Ω·m, approximately 20x larger than that for bulk silver metal. Please click here to view a larger version of this figure.

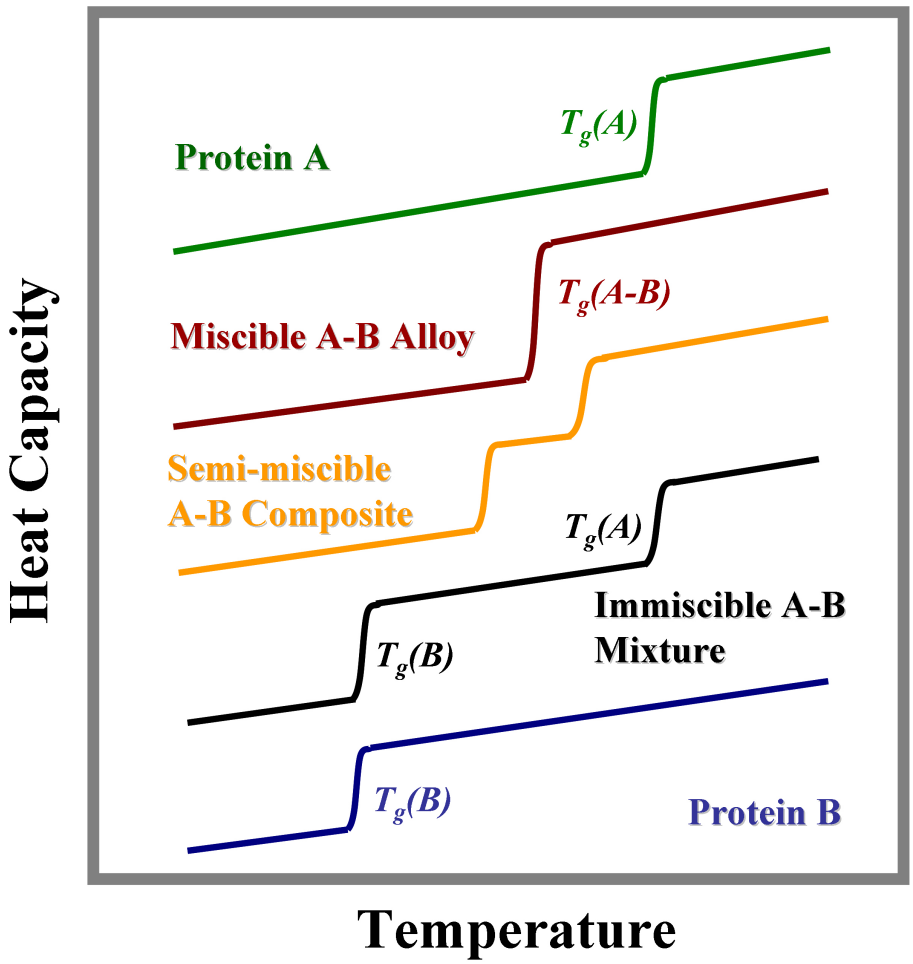

Figure 6. Thermal analysis model used for verifying miscibility of blended protein system. If protein A and B have individual single glass transition temperatures, T_g(A) and T_g(B), respectively (green and blue curves), a fully miscible protein alloy system will show only one glass transition different from the T_gs of A and B (red curve). Otherwise, the proteins are immiscible mixtures with both T_g(A) and T_g(B) (black curve), or semi-miscible composites with two shifted glass transitions (orange curve).

Discussion

One of the most critical procedures in producing "alloy" protein system is to verify the miscibility of the blended proteins. Otherwise, it is only an immiscible protein mixture or protein composite system without stable and tunable properties. An experimental thermal analysis method can be used for this purpose and to confirm their alloy properties. Protein-protein interactions can be viewed according to Flory-Huggins's lattice model[48] as interactions between the "solvent" (the predominant protein component) and the "solute" (the minor protein component). Based on this model, the free energy change during mixing between the "solvent" and the "solute" governs the miscibility of the blend[48]. Generally, there are three different degrees of miscibility: (a) fully miscible (form one-phase material macroscopically), (b) metastable (form semi-miscible phases in the material), and (c) immiscible (remain original two-phases with individual protein A and B domains)[3,48]. Correspondingly, the glass transition behaviors of a two protein system can demonstrate these differences and ideally can be expressed using a phase diagram model (**Figure 6**). For example, if protein A and B have their individual single glass transition temperatures, T_g(A) and T_g(B), respectively (**Figure 6** green and blue curves), a fully miscible protein alloy system should show only one glass transition during the heating. This single glass transition is normally intermediate between the T_gs of A and B (**Figure 6**). Otherwise, the proteins could form an immiscible blend whereby both T_g(A) and T_g(B) appear at their original positions (**Figure 6**). The proteins may also form a semi-miscible system indicated by two shifted glass transitions (**Figure 6**). A practical example of fully miscible protein "alloy" system (form one-glass transition) can be found in the DSC scans of silk-tropoelastin blend samples in **Figure 4** (thermal application)[9]. With the decrease of silk content, the glass transition temperatures (T_g) of the blends increased gradually from 178 °C (pure silk) to 190 °C (pure tropoelastin)[9], yet consistently keep a homogeneous single glass transition for all type of blends. According to Flory-Huggins's model, this indicates that all silk-tropoelastin blends of various mixing ratios are stable and are fully miscible protein alloys without any macrophase separations.

In conclusion, new generations of protein alloy materials can be produced and fabricated into different medical devices (*e.g.*, films, sutures, screws, plates, micro-needles, gels), with controlled and tunable optical, electrical, chemical, thermal, and mechanical properties. Through controlling the mixing components and ratios, various biophysical properties of protein alloy materials, such as elasticity, strength, surface roughness, surface charge, biodurability and chemical activity, can be manipulated, which could ultimately impact the tissue functions as well as the local cellular behaviors associated with these materials. Additionally, due to the nature of proteins' programmable lifetime, *in vivo* becomes a

viable platform for these alloy materials. Such advantages could provide novel options for implantable medical devices in the future where post repair surgical retrieval can be avoided. These protein alloy biomaterials would also offer a new pathway to produce medical devices with tunable biological functions and properties, and with matching tissue compliance and related needs. This article provides a general protocol review for how to fabricate these devices and would benefit both scientists and clinical doctors in multiple biomedical fields.

Disclosures

No conflicts of interest declared.

Acknowledgements

The authors thank Rowan University for support of this research. XH also thanks Dr. David L. Kaplan at Tufts University and the NIH P41 Tissue Engineering Resource Center (TERC) for previous technical trainings.

References

1. Rosenbloom, J. *et al.* Extracellular matrix 4: The elastic fiber. *FASEB J.* **7**, 1208-1218 (1993).
2. Traub, W. *et al.* On the molecular structure of collagen. *Nature.* **221**, 914–917 (1969).
3. Hu, X. *et al.* Protein-Based Composite Materials. *Materials Today.* **15**, 208-215 (2012).
4. Hardy, J. G., & Scheibel, T. R. Composite materials based on silk proteins. *Progress in Polymer Science.* **35**, 1093-1115 (2010).
5. Kidoaki, S. *et al.* Mesoscopic spatial designs of nano- and microfiber meshes for tissue-engineering matrix and scaffold based on newly devised multilayering and mixing electrospinning techniques. *Biomaterials.* **26**, 37–46 (2005).
6. Teng, W. B. *et al.* Recombinant silk-elastin like protein polymer displays elasticity comparable to elastin. *Biomacromolecules.* **10**, 3028-3036 (2009).
7. Foo, C. W. P., & Kaplan, D. L. Genetic engineering of fibrous proteins, spider dragline, silk and collagen. *Adv Drug Delivery Rev.* **54**, 1131-1143 (2002).
8. Hu, X. *et al.* Charge-Tunable Autoclaved Silk-Tropoelastin Protein Alloys That Control Neuron Cell Responses. *Adv. Funct. Mater.* **23**, 3875-3884 (2013).
9. Hu, X. *et al.* Biomaterials derived from silk-tropoelastin protein systems. *Biomaterials.* **31**, 8121-8131 (2010).
10. Hu, X. *et al.* The influence of elasticity and surface roughness on myogenic and osteogenic-differentiation of cells on silk-elastin biomaterials. *Biomaterials.* **32**, 8979-8989 (2011).
11. Hu, X. *et al.* Biomaterials from ultrasonication-induced silk fibroin−hyaluronic acid hydrogels. *Biomacromolecules.* **11**, 3178-3188 (2010).
12. Gil, E. S. *et al.* Swelling behavior and morphological evolution of mixed gelatin/silk fibroin hydrogels. *Biomacromolecules.* **6**, 3079-3087 (2005).
13. Lu, Q. *et al.* Green process to prepare silk fibroin/gelatin biomaterial scaffolds. *Macromol. Biosci.* **10**, 289-298 (2010).
14. Lu, S. *et al.* Insoluble and flexible silk films containing glycerol. *Biomacromolecules.* **11**, 143-150 (2010).
15. Mandal, B. B. *et al.* Silk fibroin/polyacrylamide semi-interpenetrating network hydrogels for controlled drug release *Biomaterials.* **30**, 2826-2836 (2009).
16. Yeo, I. S. *et al.* Collagen-based biomimetic nanofibrous scaffolds, preparation and characterization of collagen/silk fibroin bicomponent nanofibrous structures. *Biomacromolecules.* **9**, 1106-1116 (2008).
17. Holst, J. *et al.* Substrate elasticity provides mechanical signals for the expansion of hemopoietic stem and progenitor cells. *Nat. Biotechnol.* **28**, 1123-1128 (2010).
18. Omenetto, F. G., & Kaplan, D. L. New Opportunities for an Ancient Material. *Science.* **329**, 528-531 (2010).
19. Qin, G. *et al.* Mechanism of resilin elasticity. *Nature Communications.* **3**, 1003 (2012).
20. Rockwood, D. N. *et al.* Materials fabrication from Bombyx mori silk fibroin. *Nat. Protocols.* **6**, 1612-1631 (2011).
21. Wise, S. G. *et al.* Engineered tropoelastin and elastin-based biomaterials. *Adv Protein Chem Struct Biol.* **78**, 1-24 (2009).
22. Amsden, J. J. *et al.* Rapid nanoimprinting of silk fibroin films for biophotonic applications. *Adv. Mater.* **22**, 1746-1749 (2010).
23. Lawrence, B. D. *et al.* Silk film biomaterials for cornea tissue engineering. *Biomaterials.* **30**, 1299-1308 (2009).
24. Kim, D. H. *et al.* Dissolvable films of silk fibroin for ultrathin conformal bio-integrated electronics. *Nat. Mater.* **9**, 511-517 (2010).
25. Zhang, J. *et al.* Stabilization of vaccines and antibiotics in silk and eliminating the cold chain. *Proc Natl Acad Sci U S A.* **109**, 11981-11986 (2012).
26. Pritchard, E. M. *et al.* Effect of silk protein processing on drug delivery from silk films. *Macromolecular Bioscience.* **13**, 311-320 (2013).
27. Lammel, A. S. *et al.* Controlling silk fibroin particle features for drug delivery. *Biomaterials.* **31**, 4583-4591 (2010).
28. Urry, D. W. Physical chemistry of biological free energy transduction as demonstrated by elastic protein-based polymers. *J Phys Chem B.* **101**, 11007-11028 (1997).
29. Shao, Z., & Vollrath, F. Materials: Surprising strength of silkworm silk. *Nature.* **418,** 741-741 (2002).
30. Jin, H. J., & Kaplan, D. L. Mechanism of silk processing in insects and spiders. *Nature.* **424**, 1057-1061 (2003).
31. Hu, X. *et al.* Determining Beta-Sheet Crystallinity in Fibrous Proteins by Thermal Analysis and Infrared Spectroscopy. *Macromolecules.* **39**, 6161-6170 (2006).
32. Hu, X. *et al.* Dynamic Protein−Water Relationships during β-Sheet Formation. *Macromolecules.* **41**, 3939-3948 (2008).
33. Hu, X. *et al.* Microphase separation controlled beta-sheet crystallization kinetics in fibrous proteins. *Macromolecules.* **42**, 2079-2087 (2009).
34. Cebe, P. *et al.* Beating the Heat - Fast Scanning Melts Beta Sheet Crystals. *Scientific Reports.* **3**, 1130, (2013).
35. Pyda, M. *et al.* Heat Capacity of Silk Fibroin Based on the Vibrational Motion of Poly(amino acid)s in the Presence and Absence of Water. *Macromolecules.* **41**, 4786-4793 (2008).
36. Buxton, G. A. *et al.* A lattice spring model of heterogeneous materials with plasticity. *Model. Simul. Mater. Sci. Eng.* **9**, 485-497 (2001).
37. Buxton, G. A., & Balazs, A. C. Modeling the dynamic fracture of polymer blends processed under shear. *Phys. Rev. B.* **69**, 054101 (2004).
38. Kolmakov, G. V. *et al.* Harnessing labile bonds between nanogel particles to create self-Healing materials. *ACS Nano.* **3**, 885-892 (2009).

39. Duki, S. F. *et al.* Modeling the nanoscratching of self-healing materials. *J. Chem. Phys.* **134**, 084901 (2011).
40. Bell, G. I. Models for the specific adhesion of cells to cells. *Science.* **200**, 618-627 (1978).
41. Bell, G. I. *et al.* Cell adhesion. Competition between nonspecific repulsion and specific bonding. *Biophys. J.* **45**, 1051-1064 (1984).
42. Wang, Q. *et al.* Effect of various dissolution systems on the molecular weight of regenerated silk fibroin. *Biomacromolecules.* **14**, 285–289, (2013).
43. Wray, L. S., *et al.* Effect of processing on silk-based biomaterials: reproducibility and biocompatibility. *J Biomed Mater Res B Appl Biomater.* **99**, 89–101 (2011).
44. Lawrence, B. D. *et al.* Silk film culture system for *in vitro* analysis and biomaterial design. *J. Vis. Exp.* (62), e3646, DOI : 10.3791/3646 (2012).
45. Hu, X., *et al.* Regulation of Silk Material Structure by Temperature-Controlled Water Vapor Annealing. *Biomacromolecules.* **12**, 1686-1696 (2011).
46. Yucel, T. *et al.* Vortex-induced injectable silk fibroin hydrogels. *Biophys J.* **97**, 2044-2050 (2009).
47. Yucel, T. *et al.* Non-equilibrium silk fibroin adhesives. *J Struct Biol* .**170**, 406-412 (2010).
48. Flory, P. J. *Principles of polymer chemistry.* Ithaca: N.Y., Cornell University Press, (1953).
49. Chen, H. *et al.* Thermal properties and phase transitions in blends of Nylon-6 with silk fibroin. *J Therm Anal Calorim.* **93**, 201-206 (2008).
50. Scabarozi, T. H. *et al.* Epitaxial growth and electrical-transport properties of Ti7Si2C5 thin films synthesized by reactive sputter deposition, *Scripta Materialia.* **65**, 811-814 (2011).
51. Tao, H. *et al.* Silk materials-a road to sustainable high technology. *Adv Mater.* **24**, 2824-2837 (2012).
52. Annabi, N. *et al.* Cross-linked open-pore elastic hydrogels based on tropoelastin, elastin and high pressure CO2. *Biomaterials.* **31**, 1655-1665 (2010).
53. Moll, R. *et al.* The human keratins: biology and pathology. *Histochem Cell Biol.* **129**, 705–733 (2008).

